Stability Trend of Metal–Organic Frameworks with Heterometal-Modified Hexanuclear Zr Building Units

Citation: Yuan, Shuai et al. "Stability Trend of Metal–Organic Frameworks with Heterometal-Modified Hexanuclear Zr Building Units." Journal of Physical Chemistry C 123, 46 (October 2019): 28266–28274 © 2019 American Chemical Society

As Published: http://dx.doi.org/10.1021/acs.jpcc.9b08749

Publisher: American Chemical Society (ACS)

Persistent URL: https://hdl.handle.net/1721.1/128195

Version: Author's final manuscript: final author's manuscript post peer review, without publisher's formatting or copy editing

Stability Trend of Metal−Organic Frameworks with Heterometal-Modified Hexanuclear Zr Building Units

Shuai Yuan,[*,†,‡,§,∥] *Jiayu Peng,*[‡] *Yirui Zhang,*[†] *and Yang Shao-Horn**[*,†,‡,§]

[†] Department of Mechanical Engineering, Massachusetts Institute of Technology, Cambridge, MA 02139, USA

[‡] Department of Materials Science and Engineering, Massachusetts Institute of Technology, Cambridge, MA 02139, USA

[§] Research Laboratory of Electronics, Massachusetts Institute of Technology, Cambridge, MA 02139, USA

[∥] Department of Chemical Engineering, Massachusetts Institute of Technology, Cambridge, MA 02139, USA

ABSTRACT: Bimetallic MOFs based on heterometal-modified hexanuclear Zr building units have emerged as promising materials for applications in energy-related fields such as heterogenous catalysis/electrocatalysis. However, their stability remains a challenge under some practical conditions and the physical/chemical origin to the (in)stability is not well understood. Herein, we

selected three representative Zr-MOFs (MOF-808, NU-1000, UiO-66) as platforms, and incorporated different heterometals (Ti^{4+}, V^{3+}, V^{5+}, Cr^{3+}, Cr^{6+}, Mn^{2+}, Fe^{2+}, Fe^{3+}, Co^{2+}, Ni^{2+}, Cu^{2+}, and Zn^{2+}) to form a series of bimetallic M/Zr-MOFs. Their stability was examined in aqueous solutions of various pH to define their stability windows and understand their stability trend. The stability of M/Zr-MOFs was found to be dictated by the oxidation states of incorporated heterometals, and slightly affected by the supporting Zr-MOFs. Water exchange rate constant, defined as the rate constant by replacing a coordinated water with a solution water, was proposed as the stability descriptor to explain the stability trend, and guide the design and application of future stable MOFs.

1. INTRODUCTION

Metal−organic frameworks, or MOFs, are crystalline porous solids constructed by self-assembly of metal cations (or metal clusters) and organic ligands having multiple binding sites.[1] MOFs have attracted research interest in fundamental science and energy applications including hydrogen/hydrocarbon gas storage,[2-3] separation,[4] heterogeneous catalysis/electrocatalysis,[5-6] optoelectronics, and energy harvesting.[7-8] MOFs thrive on diverse structures and tunable physiochemical properties: the metals and organic ligands within MOFs can be much diversified, giving rise to unlimited framework structures.[9] Despite numerous advantages, the practical applications of MOFs are ultimately limited by their low stability towards water or aqueous solutions.[10] For example, MOF-5 (composed of Zn^{2+} and dicarboxylate linkers), a prominent milestone in MOF research, decomposes gradually upon exposure to moisture in air. When MOFs are used for certain applications, their framework integrity must be guaranteed to maintain their intended functionalities and characteristics. In fact, water or moisture is usually present in

industrial processes, thus practical applications in catalysis/electrocatalysis often require stability towards aqueous acids/bases. Therefore, the chemical stability of MOFs has been receiving increasing attention over the years.[11] Researchers have started to address the stability of MOFs in different environments, understand the possible decomposition pathways, and develop more stable framework structures. A fundamental understanding of the stability principle will guide the synthesis of stable MOFs by design and will significantly expand the application areas of MOFs.

Previous work suggests that the stability of MOFs is dictated by the metal−ligand coordination bond strength, because the coordination bonds are the most labile moieties in MOFs,[11] which is in line with the observation that high valent metal cations (such as Ti^{4+}, Zr^{4+}, Al^{3+}, Fe^{3+}, and Cr^{3+}) tend to form stable MOFs when combined with carboxylate-based linkers.[12-15] However, the effect of metal cations on the stability of MOFs have not been systematically compared according to our knowledge. The absence of systematic study is attributed to the fact that multiple factors (including the metal ions,[16] organic ligands,[17] metal−ligand coordination geometry,[18] pore size,[19] hydrophobicity,[20] etc.) may affect the stability simultaneously, which makes it exceedingly difficult to selectively study the contribution of metal cations. For example, it has been demonstrated that the moisture and water-resistant of MOFs can be enhanced by hydrophobic organic ligands[21] or hydrophobic polymer coating without changing the coordination bonds.[22] Indeed, in order to investigate the effect of metal cations, a series of isostructural MOFs with different metals and oxidation states are required. However, the change of metal cations and/or their oxidation states often alters the framework structures at the same time, which in turn changes the coordination geometry or pore structures.

Recently, considerable attention has been given to a class of bimetallic MOF bearing a $[Zr_6O_4(OH)_4]$ secondary building unit and a heterometal attaching to the Zr_6-core.[23-33] These

heterobimetallic MOFs (namely M/Zr-MOFs where M stands for heterometals) are formed by depositing heterometal cations onto the −OH groups of the Zr-clusters.[23] It has been demonstrated that different transition metals with various oxidation states can be incorporated into Zr-MOFs to form bimetallic M/Zr-MOFs.[23-33] A reprehensive example is the Zr-MOF NU-1000 (NU = Northeastern University), which acts as a platform to support a series of metal species including Al^{3+}, Zn^{2+}, In^{3+}, Ni^{2+}, Co^{2+}, $Fe^{2+/3+}$, Cu^{2+}, Mg^{2+}, Mo^{6+}, W^{6+}, Re^{7+}, etc.[23-30] Due to the exceptional robustness of Zr-based MOFs,[12] their derived M/Zr-MOFs are believed to possess high thermal and chemical stability. Furthermore, it has been recognized as a promising method to separate and stabilize single atoms or metal clusters to maximize the utilization of active metal sites.[34-35] Therefore, M/Zr-MOFs have attracted intense research interests in energy related areas including heterogenous catalysis and electrocatalysis,[23-33, 36] which usually require stable frameworks at high elevated temperature or acidic/basic aqueous solutions. For example, Co^{2+} modified NU-1000 has been shown as an excellent heterogenous catalyst for the oxidative dehydrogenation of propane.[37] Co^{2+}/NU-1000 has also been fabricated into thin films to enable electrocatalytic water oxidation.[38] In another example, deposition of MoS_x species onto Zr node of NU-1000 forms bimetallic catalysts for electrochemical hydrogen evolution.[39] Although widely studied in energy applications, the stability of M/Zr-MOFs has not been fully understood. In fact, M/Zr-MOFs provide an ideal platform to systematically study the effect of metal cations on the stability of MOFs, because they possess identical backbone structure and similar metal coordination environment but different transition metal centers. A fully understanding of the stability trend of M/Zr-MOFs will not only direct the application of this specific class of MOFs, but also extract descriptors and knowledge to guide the design of future stable MOFs. Bear this in mind, we have constructed a series of M/Zr-MOFs with different heterometals (M^{n+} = Ti^{4+}, V^{3+}, V^{5+}, Cr^{3+}, Cr^{6+},

Mn^{2+}, Fe^{2+}, Fe^{3+}, Co^{2+}, Ni^{2+}, Cu^{2+}, and Zn^{2+}) and framework structures, examined their stability in aqueous solutions of various pH, in expecting to understand the stability trend, define stability descriptors and guide the design of future stable MOFs. It has been found that the incorporated heterometals may leach from the M/Zr-MOFs, and stability of heterometal cations increase with their oxidation states. In addition, Zr-MOF-supports matrices with Zr-clusters of low connection numbers possess stronger stability than high-connected ones. Based on the observed leaching of metal and ligands under different pH environments, possible decomposition pathways are proposed for different types of M/Zr-MOFs. Finally, we define the water exchange rate constant as a stability descriptor of M/Zr-MOFs, which will be applied to direct design and application of future stable MOFs.

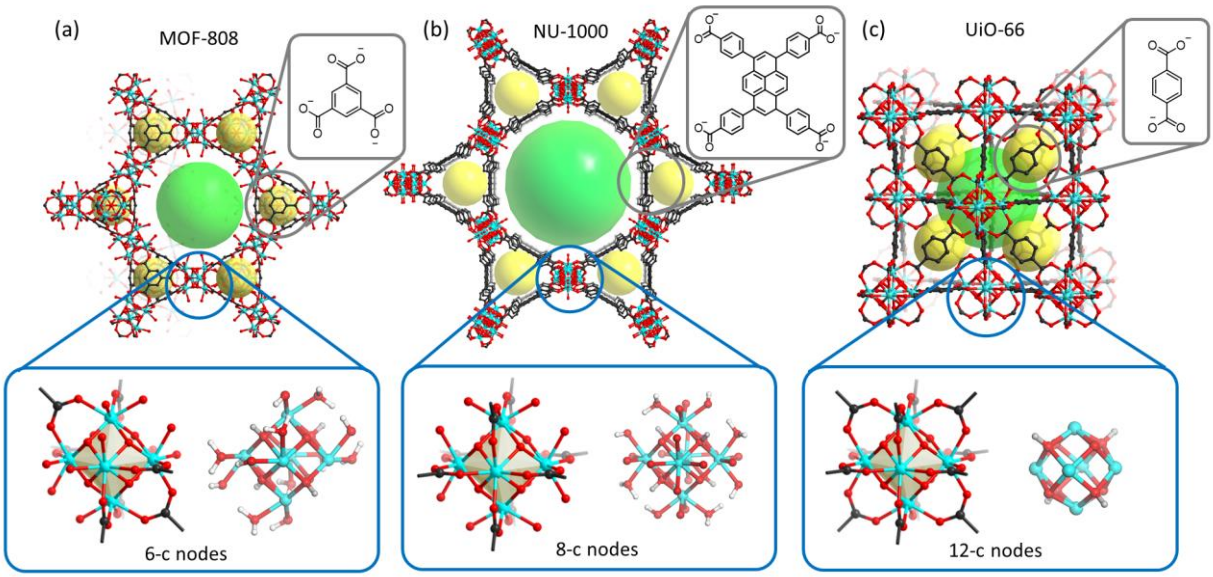

Figure 1. Structures of 12, 8, and 6-connected Zr_6-nodes in MOF-808 (a), NU-1000 (b) and UiO-66 (c). Top insert shows the structure of organic ligand; bottom insert shows the structure of 6-, 8-, 12-connected Zr_6 clusters with theoretically 22, 16, and 4 protons on each Zr_6 cluster for MOF-

808 (a), NU-1000 (b) and UiO-66 (c). Blue, red, white and black balls represent Zr, O, H and C atoms, respectively. Green and yellow spheres represent two types of pores in Zr-MOFs.

2. METHODS

Materials and Characterization. All chemicals were used as received without further purification. Gas sorption measurements were conducted using a Micrometritics ASAP 2020 system. PXRD was carried out with a Bruker D8-Focus Bragg-Brentano X-ray Powder Diffractometer equipped with a Cu sealed tube (λ = 1.54178 Å) at 40 kV and 40 mA. UV-vis absorption spectra were recorded on a Cary 5000 UV-Vis-NIR spectrophotometer. ICP-MS data were collected with an Agilent 5100 DVD inductively coupled plasma-optical emission (ICP-OES) spectrometer. MOF-808, NU-1000, UiO-66, and DUT-53 was synthesized according to the reported procedure,[12, 40-42] with slight modifications. The terminal carboxylate ligands was removed by DMF/water/acetone washing followed by thermal activation at 100 °C under vacuum, as indicated by ^{1}H-NMR of digested samples (Experimental Details, Supporting Information).

Synthesis of M/NU-1000. M/NU-1000 (M = Ti^{4+}, V^{3+}, V^{5+}, Cr^{3+}, Cr^{6+}, Mn^{2+}, Fe^{2+}, Fe^{3+}, Co^{2+}, Ni^{2+}, Cu^{2+}, and Zn^{2+}) were synthesized by incubating the crystalline powder of NU-1000 (100 mg) in the solution of $Ti(O^iPr)_4$, VCl_3, $NaVO_3$, $CrCl_2$, K_2CrO_4, $Mn(NO_3)_2$, $FeCl_2$, $Co(NO_3)_2$, $Ni(NO_3)_2$, $Cu(NO_3)_2$, or $Zn(NO_3)_2$, respectively (Experimental Details, Supporting Information).

Stability Test. M/Zr-MOFs (10 mg) were incubated in 20 mL aqueous solution of different pH for 1 h (pH was adjusted by NaOH and HCl). The solids were separated by centrifugation. The solutions were neutralized and filtered through 0.2 μm filter before UV-vis and ICP-OES test. The solids were dissolved in J.T. Baker Ultrex® II Ultrapure 70% nitric acid at 70 ºC for 12 hours. Each

solid sample was prepared in triplicate to maintain accuracy of ICP-OES analysis. Calibration standards were prepared from certified reference standards from RICCA Chemical Company. Resulting calibration curves have minimum $R^2 = 0.9999$. The individual results of the triplicate samples were averaged to determine the metal ratios.

3. RESULTS AND DISCUSSION

Synthesis of M/Zr-MOFs. Three representative Zr-based MOFs, namely MOF-808,[40] NU-1000[41] and UiO-66[12] (UiO = University of Oslo), were selected as matrices, because they have varying node connectivity and thereby different interactions with attached metal cations. Their metal nodes bear the same $[Zr_6O_4(OH)_4]$ core but different connection numbers with carboxylate ligands. Each Zr_6 cluster in MOF-808 is connected to six carboxylates from organic ligands, leaving the rest six sites occupied by terminal $-OH_2$/OH groups (Figure 1a). NU-1000 has Zr_6 clusters coordinated to eight carboxylates with four coordinatively unsaturated Zr^{4+}-sites, each terminated by a pair of $-OH_2$/OH group (Figure 1b). UiO-66 possess Zr_6 clusters connected to 12 carboxylates although the connection number is usually reduced to ~11 due to the existence of intrinsic defects (Figure 1c).[43] The terminal $-OH_2$/OH groups on the coordinatively unsaturated sites of Zr_6 clusters act as anchors to bind with heterometal cations. Therefore, the connectivity of Zr_6 clusters will affect the amount of the attached metal cations and their binding affinity.

In this work, different metal cations (M^{n+}) including Ti^{4+}, V^{3+}, V^{5+} (VO_4^{3-}), Cr^{3+}, Cr^{6+}(CrO_4^{2-}), Mn^{2+}, Fe^{2+}, Fe^{3+}, Co^{2+}, Ni^{2+}, Cu^{2+}, and Zn^{2+} were introduced into NU-1000 to form M/NU-1000 bimetallic materials. Similarly, Fe^{3+}/UiO-66 and Fe^{3+}/MOF-808 were synthesized from UiO-66 and MOF-808 respectively. Among these MOFs, NU-1000 is widely studied as a platform to incorporate heterometals for heterogenous catalysis/electrocatalysis because of its high chemical

stability and hierarchically micro-mesoporous structure.[23-30] Generally, M/Zr-MOFs were synthesized using a two-step method. The parent Zr-MOFs were initially synthesized by the self-assembly of the Zr^{4+} with respective carboxylate-based linkers under solvothermal conditions. Further treatment of as-synthesized Zr-MOFs with the solutions of transition metal cations (M^{n+}) leads to the formation of bimetallic M/Zr-MOFs by attaching the metal cations on the terminal $-OH_2$/OH groups. During this process, the active protons from terminal $-OH_2$/OH groups on Zr_6 clusters were replaced by heterometal cations to form bimetallic clusters. The V^{5+} (VO_4^{3-}) and Cr^{6+} (CrO_4^{2-}) were incorporated using their respective metalates (i.e. Na_3VO_4 and K_2CrO_4), which undergoes a different reaction mechanism. High valent metals tend to exist in the form of anionic metalates in the solutions, which directly coordinate to the Zr-sites by replacing the terminal $-OH_2$/OH groups. The chemical equation representing the stepwise synthesis of M/Zr-MOFs are illustrated in Figure 2. It should be noted that the proton assignments within these metal nodes are not clear, although simulations indicate that $-O^{2-}$, $-OH^-$ and $-H_2O$ are interconvertible by rapid proton transfers.[44]

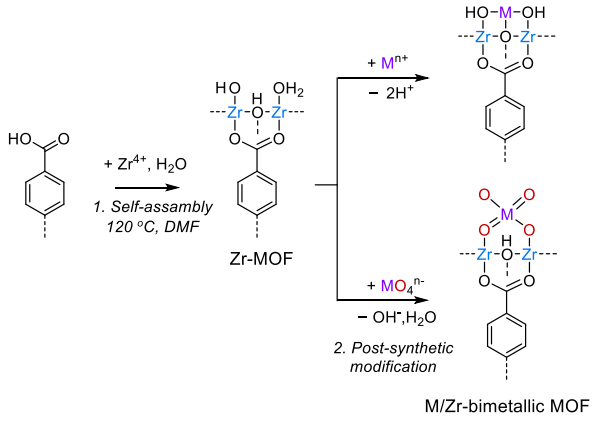

Figure 2. Schematic representation showing the two-step synthesis of M/Zr-MOFs. The attachment of metal cations and metalates occurs by replacing H^+ and OH^- respectively. The

scheme do not reflect the real stoichiometry of reactions. The ratios between carboxylate linkers, Zr, M, and H^+ differ depending on the Zr-MOF structure and M species. M^{n+} = Ti^{4+}, V^{3+}, V^{5+} (VO_4^{3-}), Cr^{3+}, Cr^{6+}(CrO_4^{2-}), Mn^{2+}, Fe^{2+}, Fe^{3+}, Co^{2+}, Ni^{2+}, Cu^{2+}, and Zn^{2+}.

The compositions of the resulting M/Zr-MOFs were analyzed by inductively coupled plasma atomic emission spectroscopy (ICP-OES). The M/Zr ratios varied from 10.2% to 44.7% depending on the synthetic conditions, acidity of heterometal species, and the structures of MOF-matrices (Table S1). Mn^{2+}/Ni^{2+}/Co^{2+}/NU-1000 are synthesized under similar synthetic conditions but different M/Zr ratios were observed (15.4% for Mn^{2+}; 22.6% for Ni^{2+}; 44.7% for Co^{2+}), possibly due to different acidity of metal cations (pK_a = 11.5 for Mn^{2+}; 10.6 for Ni^{2+}; 10.0 for Co^{2+}). More acidic metal cations are expected to easily replace H^+ on the terminal $-OH_2$/OH group during metalation process. A comparison of different MOF matrices indicates the dependence of metal loading on the connection number of Zr_6-nodes: Zr_6-nodes with low connection number and more terminal $-OH_2$/OH groups tend to accommodate more metal cations. This trend is supported the Fe/Zr ratios of Fe^{3+}-MOF-808 (10.7%), Fe^{3+}-NU-1000 (28.3%), and Fe^{3+}-UiO-66 (32.8%, Table S1).

This trend is consistent with the proposed reaction mechanism that the metal cations replace the H^+ from terminal $-OH_2$/OH groups upon binding.[23-30] The phase purity of as-synthesized Zr-MOFs and M/Zr-MOFs was confirmed by PXRD patterns (Figure S1, S2), which match well with the simulations based on the crystal structures. M/Zr-MOFs show almost identical diffraction patterns as their respective parent Zr-MOFs, indicating the unaltered framework structures after metal deposition. Their porous structures were further confirmed by N_2 adsorption/desorption isotherms at 77 K (Figure S3). Taking Fe^{3+} incorporated Zr-MOFs as examples, Fe^{3+}/MOF-808, Fe^{3+}/NU-1000, and Fe^{3+}/UiO-66 remain porous with slightly decreased total N_2 uptakes and BET surface

areas compared to their parent structures (Table S2). The reduced porosity can be attributed to the increased molecular weight and partially occupied pore spaces after metal deposition. The attachment of metal species onto the terminal −OH groups of Zr_6 clusters was further confirmed by Fourier transform infrared (FT-IR) spectra (Figure S4). The peak corresponding to O–H stretches of terminal −OH group at 3672 cm^{-1} decreased upon the incorporation of Co^{2+} or Cr^{6+}, which is in agree with the proposed metalation mechanism. The ICP-OES data, PXRD patterns, N_2 adsorption, and FT-IR measurements unambiguously confirmed the successful synthesis of M/Zr-MOFs.

Stability Test of M/Zr-MOFs. The stability test of Zr-MOF and M/Zr-MOFs was carried out by incubating MOF samples in aqueous solutions at pH from 0 to 14 for 1 h. After separating the remaining solids by centrifugation, the crystallinity of the MOF-solids was assessed by PXRD while the leaching of metals and organic ligands in the solution was detected by ICP-OES and UV-vis spectra, respectively. PXRD showed that the parent Zr-MOF (MOF-808) was stable within the pH range of 0 to 12, whereas amorphization began above pH 12 (Figure S5a). The supernatants of MOF samples in aqueous solutions after the stability test were also analyzed by ICP-OES and UV-vis, indicating comparable stability for MOF-808, NU-1000, and UiO-66. UV-vis did not observe the adsorption peaks of corresponding ligand for MOF-808, NU-1000, and UiO-66 between pH = 0 to 11, whereas ligand leaching was found at pH = 12 and higher. The stability of Zr-MOF in this pH range is further supported by no significant leaching or soluble Zr^{4+} detected in the solution over the pH range of 1 to 12 (Figure 3a). On the other hand, the instability of Zr-MOFs above pH 12 was accompanied by the absence of soluble Zr^{4+} by ICP-OES analysis of supernatants (Figure 3b), which can be attributed to the formation of zirconium oxide/hydroxide solids at pH greater than 12.[45] Since the stability of M/Zr-MOFs are not expected to exceed their

parent Zr-MOFs, the stability test of all M/Zr-MOFs was conducted within the pH window of 0 to 12.

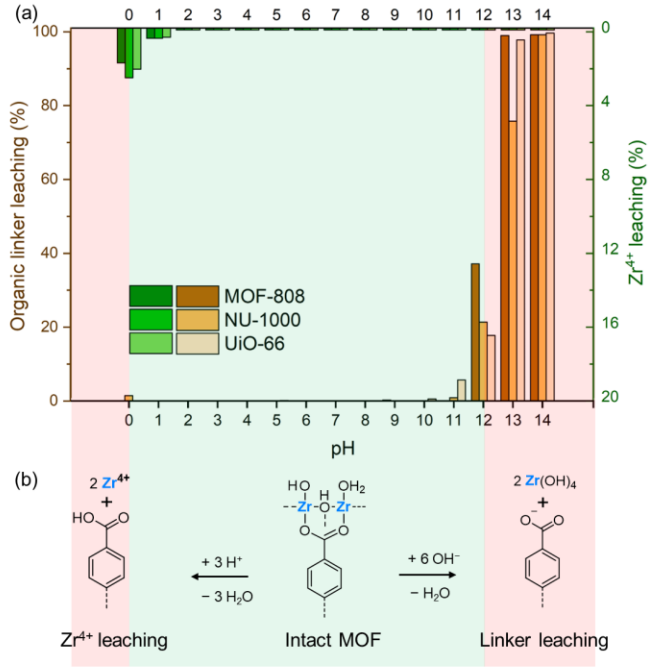

Figure 3. (a) Leaching organic linkers (yellow) and Zr^{4+} (green) from MOF-solids to solutions after the treatment of aqueous solution of various pH. The organic linkers and Zr^{4+} in the supernatant were monitored by UV-vis and ICP-OES, respectively to calculate the linker and Zr^{4+} remaining ratios in solids. MOF-808, NU-1000, and UiO-66 show comparable stability within the pH range of 0-12. The concentration or organic linkers with in pH range of 1-10 and the concentration of Zr^{4+} with in the pH range of 1-14 were below detection limit of UV-vis and ICP-OES. (b) Corresponding proposed decomposition mechanisms of Zr-MOFs in acid and base. The scheme do not reflect the real stoichiometry of reactions. The H^+ assignment and the ratios between carboxylate linkers, Zr, and H^+ differ depending on the Zr-MOF structure.

The heterometals attached to the Zr_6 cluster are not directly coordinated to the organic ligands in M/Zr-MOFs, thereby do not alter the stability of Zr-MOF-backbones, which was confirmed by PXRD, ICP-OES and UV-vis spectra. Taking Co^{2+}/MOF-808 as an example, PXRD of Co^{2+}-MOF-808 was unaltered within a pH range of 0-12, suggesting the maintained backbone structure. The leaching of Zr^{4+} and organic linker for Co^{2+}/MOF-808 was found comparable to that of parent MOF-808 within a pH range of 0-12, implying a stable framework structure. However, an obvious color change was observed for Co^{2+}/MOF-808 in pH=0, an indication of significant Co^{2+} leaching (Figure S5b). The precise composition of Co^{2+}/MOF-808 solid after the stability test was analyzed by ICP-OES of digested MOF samples, which showed neglectable Co^{2+} remaining in the solid (Figure S5c). Since no obvious Zr^{4+} leaching was observed during the stability test, the leaching of Co^{2+} was calculated from the Co/Zr ratios in the solid. Using a similar method, the compositions of different M/Zr-MOFs under varying pH were examined and compared in Figure 4.

We first compared the stability of different metal cations anchored onto NU-1000. The stability of M/Zr-NU-1000 under different pHs are strongly affected by the valence of incorporated metals (Figure 4). We define the stable window as the pH range under which over 80% of heterometals are remained in M/Zr-MOF solids. Low valent metal cations (Mn^{2+}, Fe^{2+}, Co^{2+}, Ni^{2+}, Cu^{2+}, and Zn^{2+}) were only stable under basic environments (pH = 12 to 11), whereas decreasing of pH was accompanied with significant metal leaching (Figure 4a top). This observation is in line with the formation mechanism of these M/Zr-MOFs, in which active protons from Zr_6 nodes are replaced by M^{n+} under basic conditions.[23-30] Increasing the concentration of H^+ will increase the driving force of H+ to replace M^{2+}, therefore reverse the metalation process, causing the detachment of metal cations from bimetallic M/Zr clusters. The stability windows of Zr-MOFs with all the divalent cations were found comparable. Fe^{2+}/Ni^{2+}/Co^{2+}/NU-1000 appeared to have slightly

greater stability than Cu^{2+}/Zn^{2+}/Mn^{2+}/NU-1000, which difference can be attributed to the relatively stronger crystal field stabilization energy of d^6 (Fe^{2+}), d^7 (Co^{2+}) and d^8 (Ni^{2+}) configurations in octahedral coordination geometry. Increasing the valence state of metal cations from 2+ to 3+ or 4+ greatly increased its stability in Zr-MOFs (Figure 4a bottom), where Zr-MOFs with Ti^{4+}, V^{3+}, Cr^{3+}, and Fe^{3+} were found stable in alkaline and neutral environments but metal leaching was found to occur in acid. Cr^{3+} appeared to exhibit the highest stability within a pH range of 0 to 11, which is comparable to parent Zr-MOF. The reaction equation of metal leaching from M/NU-1000 are shown in Figure S6a. According to the equation, the concentration of a metal cation in the solution should be linearly related to $[H^+]^n$, where $[H^+]$ is the concentration of proton in the solution and n is the charge of the metal cation. The concentration of metal in the solution with different pHs measured from ICP-OES in the logarithmic scale with the H^+ concentration in the solution was largely linear, where the slope (0.088 for Co^{2+}, 0.16 for V^{3+}, 0.20 for Ti^{4+} obtained by linear regression) is proportional to the charge of metal cations (Figure S6b). Further increasing the valence state of metal ions to 5+ and 7+ (i.e. V^{5+} and Cr^{6+}) led to MOFs stable only under neutral conditions but unstable under strong acidic and basic conditions (Figure 4b), where the anionic metalates (VO_4^{3-} and CrO_4^{2-}) can either be protonated by H^+, or replaced by OH^-.[46]

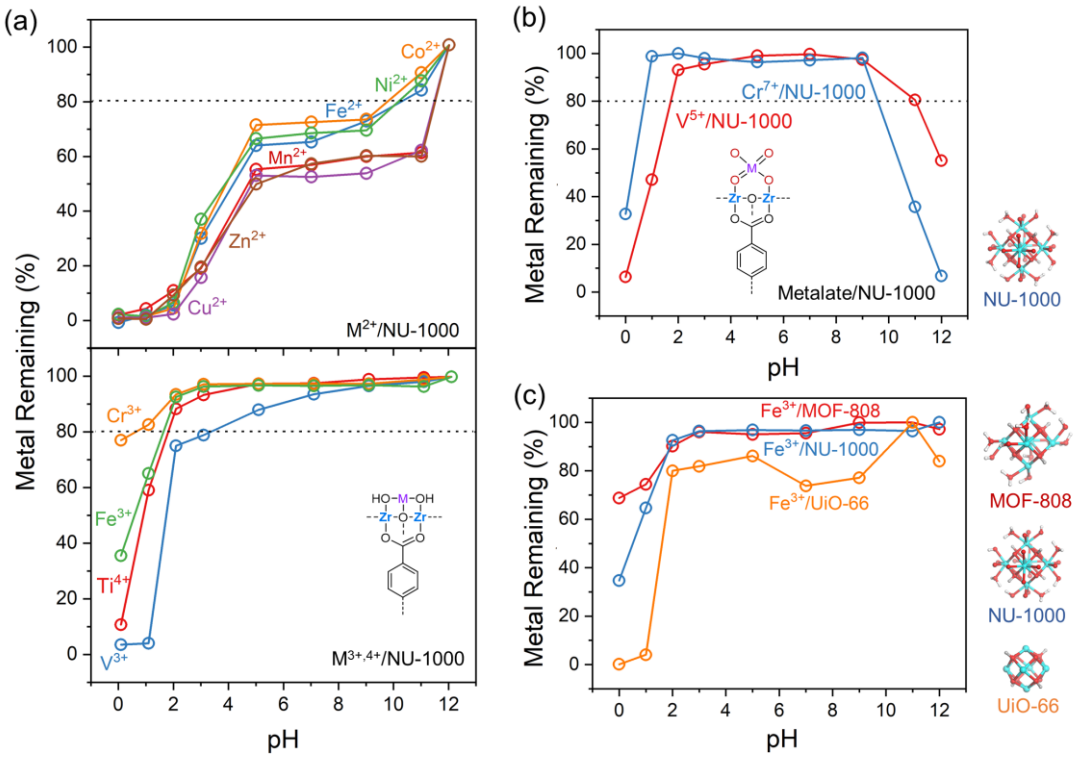

Figure 4. Stability test of M/Zr-MOFs monitored by ICP-OES. (a) Stability of metal cations in M/NU-1000 (M^{n+} = Ti^{4+}, V^{3+}, Cr^{3+}, Fe^{3+}, Mn^{2+}, Fe^{2+}, Co^{2+}, Ni^{2+}, Cu^{2+}, and Zn^{2+}); (b) stability of metalates (VO_4^{3-} and CrO_4^{2-}) in M/NU-1000; (c) a comparison of stability for Fe^{3+}/MOF-808, Fe^{3+}/NU-1000, and Fe^{3+}/UiO-66. Insert shows the structural model of Zr_6 clusters in respective MOFs. The stability test was carried out by incubating 10 mg M/Zr-MOFs in 20 mL aqueous solution of different pH for 1 h (pH was adjusted by NaOH and HCl). The solids were collected, digested, and analyzed by ICP-OES to obtain M/Zr ratio. The remaining metals in solids after stability test was calculated by comparing the M/Zr ratio with that of as-synthesized M/Zr-MOF.

The effects of different Zr-MOF motifs on the stability of incorporated metals were further examined. As an example to show the stability difference, Fe^{3+} substituted onto Zr-MOF-808 and NU-1000 were more stable than that in UiO-66 (Figure 4c). The lower metal leaching of Fe^{3+}-

MOF-808 and NU-1000 can be attributed to the fact that Zr_6 cluster low carboxylate connection numbers (i.e. with more terminal $-OH_2/OH$) stabilizes the attached metals, which is supported by previous work having Zr_6 cluster possess more terminal $-OH_2/OH$ are more prone to deprotonate to bind with Fe^{3+},[47] and less likely to be protonated to cause Fe^{3+} leaching. The connection number of Zr_6 clusters in UiO-66 is almost 12-connected, leaving limited $-OH_2/OH$ to stabilize Fe^{3+}. In addition, multiple terminal $-OH_2/OH$ groups from Zr_6 cluster with low connection numbers may binds to a Fe^{3+} simultaneously, stabilizing Fe^{3+} by chelating effects.[26] To further confirm the effect of connection numbers on the stability, a Zr-MOF with 8-connected Zr_6 cluster, namely DUT-53,[42] was selected to form bimetallic Fe^{3+}/DUT-53. Bearing the same type of 8-connected Zr_6 clusters, Fe^{3+}/DUT-53 and Fe^{3+}/NU-1000 shows comparable stability (Figure S7). The slightly higher stability of Fe^{3+}/NU-1000 was tentatively attributed to its more rigid framework. It should be noted that different metal cations with various M/Zr ratios may possess distinct binding modes with the Zr_6 supports, which may also affect their stability. But this will not be discussed herein since the local structure of heterometal cations on the M/Zr-MOFs was not the focus of this work.

Based on the experimental observations, decomposition mechanisms of M/Zr-MOFs in acid and base are proposed here. In acid, M/Zr-MOFs undergo a two-step decomposition pathway, which can be viewed as a reverse process of the MOF formation (Figure 5a). For metal cations attached Zr-MOFs, the relatively labile M−O coordination bond will be initially dissociated by H^+ attack, leading to the detachment of M^{n+}. Further increasing the H^+ concentration will subsequently break the strong Zr−O bond and dissolve the whole material. In base, the carboxylate ligands will be replaced by OH^-, leading to the leaching of organic ligands while generating metal oxide/hydroxide solids. For metalates attached Zr-MOFs, the decomposition can happen in both acidic and basic environments (Figure 5b). As an anion, metalates can be replaced by $-OH^-$ or

protonated by H^+, leading to the metal leaching. These mechanisms are supported by the stability trends of M/Zr-MOFs observed in this study, which are discussed in detail below.

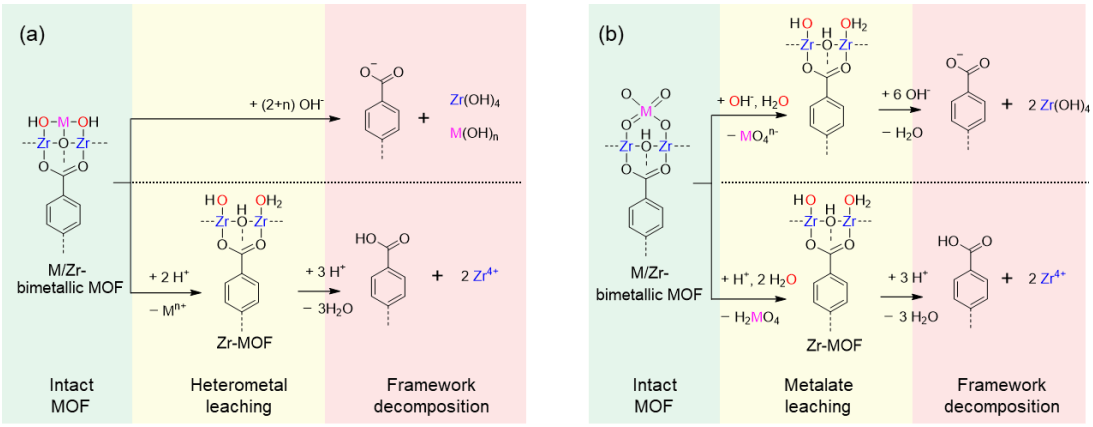

Figure 5. Schematic representation of decomposition mechanisms of M/Zr-MOFs in acid and base. (a) Low-valent-metal-based M/Zr-MOF (M = Ti^{4+}, V^{3+}, Cr^{3+}, Fe^{3+}, Mn^{2+}, Fe^{2+}, Co^{2+}, Ni^{2+}, Cu^{2+}, and Zn^{2+}) decompose into carboxylate and metal hydroxide in base. In low concentration acid, heterometals will leach. In high concentration acid, Zr^{4+} will leach causing the framework decomposition. (b) High valent metal (V^{5+} and Cr^{6+}) leach from M/Zr-MOFs as metalates in base or protonated forms in acid. Further increasing of base or acid concentration cause the decomposition of Zr-MOF. The scheme do not reflect the real stoichiometry of reactions. The H^+ assignment and the ratios between carboxylate linkers, Zr, M and H^+ differ depending on the Zr-MOF structures and the M species.

The dissociation of relatively labile M−O bond is believed to be responsible for the decomposition of M/Zr-MOFs. Low-valent metal cations form weak M−O bonds, which are vulnerable to the attack of H^+ in the solution. Increasing the valency will greatly strengthen the M−O bond owing to the enhanced columbic interactions. As a result, the high valent metal cations such as Ti^{4+}, V^{3+}, Cr^{3+}, and Fe^{3+} bind strongly with Zr-MOF backbone. For example, oxidizing

Fe^{2+}/NU-1000 into Fe^{3+}/NU-1000 significantly extended its stability window from pH = 11-12 to pH = 2-12. The valency of metalates also affects their stability. Compared with V^{5+} (VO_4^{3-}), Cr^{6+}(CrO_4^{2-}) are more stable in acid but less stable in base, due to its higher valency. Indeed, high valent chromates are less basic than vanadate, which are less likely to be protonated in acidic solutions. The stability pH window of M/NU-1000 are summarized in Figure S8. Possible operational conditions and application scopes of M/Zr-MOFs can be predicted based on their stability window. Divalent-metal-based M/Zr-MOFs possess narrow operational pH window, which is not suitable for catalysis/electrocatalysis in aqueous solutions. To be applied in aqueous environments, high valent metal species are usually required. It should be noted that while the incubation time for stability test was set to 1 h to differentiate the stability range of different M/Zr-MOFs and define their stability trend in this work, practical applications may require more harsh conditions during longer exposure time.

Descriptor of M/Zr-MOFs Stability in Acid and Base. The pK_a of hydrated metal cations $[M(H_2O)_m]^{n+}$[48] and water exchange rate constant (k_{ex}) of metal cations[49] were examined as descriptors of stability. Water exchange rate constant of a metal cation is defined as the rate constant by replacing a coordinated water on the cation with water in the solution. Correlations were both observed when plotting the lowest stable pH of M/Zr-MOFs against the pK_a of hydrated metal cations $[M(H_2O)_m]^{n+}$ or water exchange rate constant of M^{n+} (logarithmic scale). Simple linear regressions of two plots give comparable Pearson correlation coefficients (0.88 for Figure 6a and 0.92 for Figure 6b). Based on the definition of pK_a and k_{ex}, pK_a of hydrated metal cations $[M(H_2O)_m]^{n+}$ reflects the bond strength of O−H bonds (Figure 7a), whereas k_{ex} describes the inertness of M−O bonds (Figure 7b). The leaching of heterometals from M/Zr-MOF is caused by the dissociation of M−O bond, a similar process as water exchange reaction (Figure 7c). Therefore,

the lowest stable pH, as a reflection of dissolution rate constant (k_d) of M/Zr-MOFs, should correlate to the k_{ex}. In fact, the k_{ex} and pK_a are also related, as strong M−O bonds within $[M(H_2O)_m]^{n+}$ are expected to polarize O−H by inductive effect, making the O−H bond easier to dissociate. As the water exchange rate constant for metal cations have been well-documented, it can be readily used as a descriptor to roughly predict the stability of MOFs.

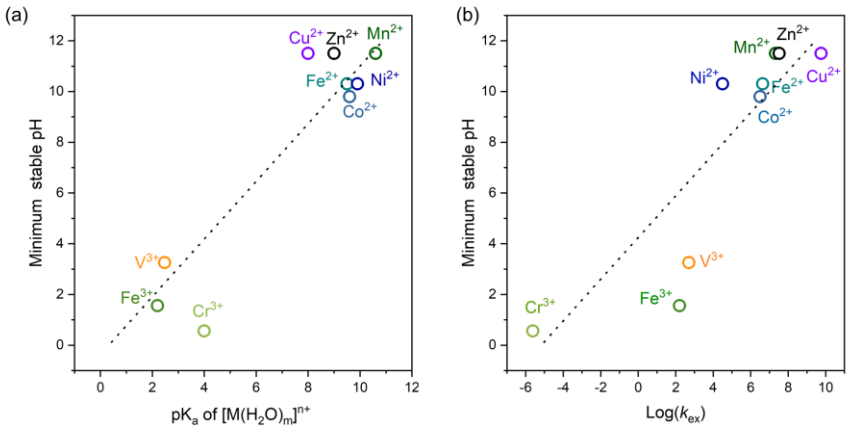

Figure 6. The relationship between the lowest stable pH and pK_a of hydrated metal cations $[M(H_2O)_m]^{n+}$ for M/NU-1000. The relationship between the lowest stable pH and water exchange rate constant of metal cations (k_{ex}) for M/NU-1000 (M^{n+} = V^{3+}, Cr^{3+}, Fe^{3+}, Mn^{2+}, Fe^{2+}, Co^{2+}, Ni^{2+}, Cu^{2+}, and Zn^{2+}). The lowest stable pH was defined as the pH under which over 80% of heterometals are remained in M/NU-1000 solids. The values of pK_a and k_{ex} were taken from previous literature.[48, 50]

Guided by this principle, the development of stable MOFs can be directed. According to the water exchange rate, increasing the oxidation states of metal cations, either in a one pot synthesis or post-synthetically, is a valid method stabilize MOFs. Among the first-row transition metal cation, Cr^{3+} and Co^{3+} show the lowest water exchange rate. Cr^{3+}-based MOF have already been

demonstrated as one of the most stable class of MOFs.[14, 51] However, reports of Co^{3+}-MOFs are still rare, possibly due to their highly oxidative nature, which tends to react with common solvents during solvothermal synthesis. Post-synthetic oxidation of suitable Co^{2+} based MOFs might be required to obtain stable Co^{3+} based MOFs. For the first-row divalent metals, V^{2+} is an outlier with unexpected high-water exchange rate constant, which may give rise to stable MOFs but has been overlooked by MOF field. Furthermore, a greater exploration of third-row transition metals, such as Ir^{3+}, $Rh^{2/3+}$, $Ru^{2/3+}$, and Pt^{2+}, may lead to the discovery of more stable MOFs. More importantly, the stability of MOFs has been found to be dictated by the oxidation states of metal cations, which provides a way to stabilize MOFs by increasing its metal oxidation states. For example, oxidation of Fe^{2+}/NU-1000 into Fe^{3+}/NU-1000 have been demonstrated to dramatically increase its stability. This concept may extend the application scopes of MOFs in electrocatalysis, because the oxidation state of metals in MOFs can be tuned by varying the electrode potential. For instance, the electrochemical oxidation of Co^{2+} to Co^{3+} on an electrode may extend the operation window pH of Co/Zr-MOFs, making them suitable for electrocatalysis. We expect that as high-valent MOFs with unknown high stability can be *in-situ* generated and stabilized on the cathodically polarized electrode, which can hardly be synthesized by traditional method. Although being a facile method to predict the stability of MOFs, potential limitations of k_{ex} as a stability descriptor still exist. For example, the coordinating groups of organic ligands (e.g. carboxylate, azolate, or pyridyl) can strongly affect the stability of MOFs, which is not described by k_{ex}. In addition, it cannot be applied to high valent metal cations that tend to hydrolysis in water (such as Ti^{4+}).

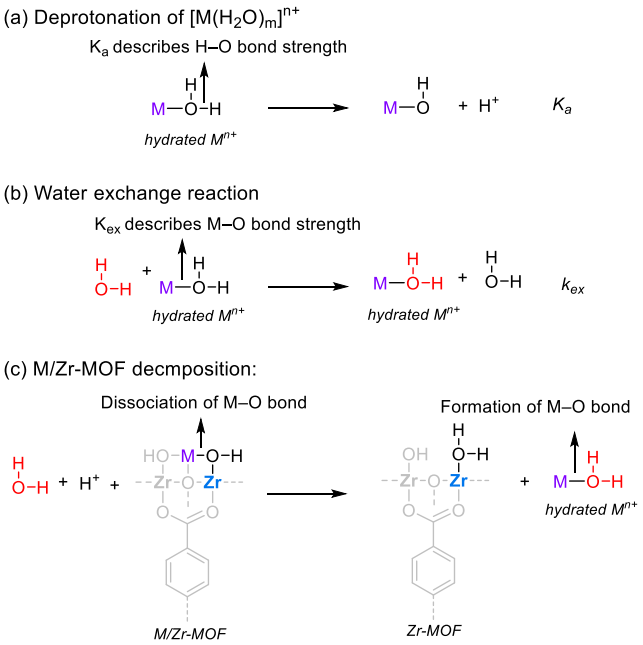

Figure 7. Simplified chemical equation representing deprotonation of $[M(H_2O)_m]^{n+}$ (a), water exchange (b), and M/Zr-MOF decomposition (c).

4. CONCLUSIONS

In conclusion, a series of M/Zr-MOFs with different heterometals (M^{n+} = Ti^{4+}, V^{3+}, V^{5+}, Cr^{3+}, Cr^{6+}, Mn^{2+}, Fe^{2+}, Fe^{3+}, Co^{2+}, Ni^{2+}, Cu^{2+}, and Zn^{2+}) have been synthesized, and their stability has been examined in aqueous solutions of various pH. Based on the stability trend, water exchange rate constant has been proposed as a stability descriptor of M/Zr-MOFs. Metal cations with higher water exchange rate constant tend to form more stable MOFs. This work has clarified the stability and possible operational conditions of M/Zr-MOFs, which will direct the exploration of applications in energy related fields including heterogenous catalysis and electrocatalysis. Furthermore, the understanding of stability trend will be applied to guide the discovery of future stable MOFs.

ASSOCIATED CONTENT

Supporting Information Supporting information of detailed material synthesis, PXRD, N2 adsorption isotherms, BET surface areas, and ICP-OES results.

The following files are available free of charge.

Supporting Information (PDF)

AUTHOR INFORMATION

Corresponding Author

*E-mail: syuansdu@mit.edu (S.Y.)

*E-mail: shaohorn@mit.edu (Y.S-H.)

Author Contributions

The manuscript was written through contributions of all authors. All authors have given approval to the final version of the manuscript.

ACKNOWLEDGMENT

This work was supported by the Toyota Research Institute through the Accelerated Materials Design and Discovery program.

REFERENCES

(1) Li, H.; Eddaoudi, M.; O'Keeffe, M.; Yaghi, O. M., Design and Synthesis of an Exceptionally Stable and Highly Porous Metal-Organic Framework. *Nature* **1999**, *402*, 276-279.
(2) Rosi, N. L.; Eckert, J.; Eddaoudi, M.; Vodak, D. T.; Kim, J.; O'Keeffe, M.; Yaghi, O. M., Hydrogen Storage in Microporous Metal-Organic Frameworks. *Science* **2003**, *300*, 1127-1129.
(3) Mason, J. A.; Oktawiec, J.; Taylor, M. K.; Hudson, M. R.; Rodriguez, J.; Bachman, J. E.; Gonzalez, M. I.; Cervellino, A.; Guagliardi, A.; Brown, C. M., et al., Methane Storage in Flexible Metal–Organic Frameworks with Intrinsic Thermal Management. *Nature* **2015**, *527*, 357.

(4) Bloch, E. D.; Queen, W. L.; Krishna, R.; Zadrozny, J. M.; Brown, C. M.; Long, J. R., Hydrocarbon Separations in a Metal-Organic Framework with Open Iron(II) Coordination Sites. *Science* **2012**, *335*, 1606-1610.
(5) Zhao, S.; Wang, Y.; Dong, J.; He, C.-T.; Yin, H.; An, P.; Zhao, K.; Zhang, X.; Gao, C.; Zhang, L., et al., Ultrathin Metal–Organic Framework Nanosheets for Electrocatalytic Oxygen Evolution. *Nat. Energy.* **2016**, *1*, 16184.
(6) Cheng, W.; Zhao, X.; Su, H.; Tang, F.; Che, W.; Zhang, H.; Liu, Q., Lattice-Strained Metal–Organic-Framework Arrays for Bifunctional Oxygen Electrocatalysis. *Nat. Energy.* **2019**, *4*, 115-122.
(7) Zhang, T.; Lin, W., Metal-Organic Frameworks for Artificial Photosynthesis and Photocatalysis. *Chem. Soc. Rev.* **2014**, *43*, 5982-5993.
(8) So, M. C.; Wiederrecht, G. P.; Mondloch, J. E.; Hupp, J. T.; Farha, O. K., Metal–Organic Framework Materials for Light-Harvesting and Energy Transfer. *Chem. Commun.* **2015**, *51*, 3501-3510.
(9) Lu, W.; Wei, Z.; Gu, Z.-Y.; Liu, T.-F.; Park, J.; Park, J.; Tian, J.; Zhang, M.; Zhang, Q.; Gentle Iii, T., et al., Tuning the Structure and Function of Metal-Organic Frameworks Via Linker Design. *Chem. Soc. Rev.* **2014**, *43*, 5561-5593.
(10) Wang, C.; Liu, X.; Keser Demir, N.; Chen, J. P.; Li, K., Applications of Water Stable Metal-Organic Frameworks. *Chem. Soc. Rev.* **2016**, *45*, 5107-5134.
(11) Yuan, S.; Feng, L.; Wang, K.; Pang, J.; Bosch, M.; Lollar, C.; Sun, Y.; Qin, J.; Yang, X.; Zhang, P., et al., Stable Metal–Organic Frameworks: Design, Synthesis, and Applications. *Adv. Mater.* **2018**, *30*, 1704303.
(12) Cavka, J. H.; Jakobsen, S.; Olsbye, U.; Guillou, N.; Lamberti, C.; Bordiga, S.; Lillerud, K. P., A New Zirconium Inorganic Building Brick Forming Metal Organic Frameworks with Exceptional Stability. *J. Am. Chem. Soc.* **2008**, *130*, 13850-13851.
(13) Dan-Hardi, M.; Serre, C.; Frot, T.; Rozes, L.; Maurin, G.; Sanchez, C.; Férey, G., A New Photoactive Crystalline Highly Porous Titanium(IV) Dicarboxylate. *J. Am. Chem. Soc.* **2009**, *131*, 10857-10859.
(14) Férey, G.; Mellot-Draznieks, C.; Serre, C.; Millange, F.; Dutour, J.; Surblé, S.; Margiolaki, I., A Chromium Terephthalate-Based Solid with Unusually Large Pore Volumes and Surface Area. *Science* **2005**, *309*, 2040-2042.
(15) Yuan, S.; Qin, J.-S.; Xu, H.-Q.; Su, J.; Rossi, D.; Chen, Y.; Zhang, L.; Lollar, C.; Wang, Q.; Jiang, H.-L., et al., [$Ti_8Zr_2O_{12}(COO)_{16}$] Cluster: An Ideal Inorganic Building Unit for Photoactive Metal–Organic Frameworks. *ACS Cent. Sci.* **2018**, *4*, 105-111.
(16) Zuluaga, S.; Fuentes-Fernandez, E. M. A.; Tan, K.; Xu, F.; Li, J.; Chabal, Y. J.; Thonhauser, T., Understanding and Controlling Water Stability of MOF-74. *Journal of Materials Chemistry A* **2016**, *4*, 5176-5183.
(17) Øien-Ødegaard, S.; Bouchevreau, B.; Hylland, K.; Wu, L.; Blom, R.; Grande, C.; Olsbye, U.; Tilset, M.; Lillerud, K. P., UiO-67-Type Metal–Organic Frameworks with Enhanced Water Stability and Methane Adsorption Capacity. *Inorg. Chem.* **2016**, *55*, 1986-1991.
(18) Song, X.; Kim, T. K.; Kim, H.; Kim, D.; Jeong, S.; Moon, H. R.; Lah, M. S., Post-Synthetic Modifications of Framework Metal Ions in Isostructural Metal–Organic Frameworks: Core–Shell Heterostructures via Selective Transmetalations. *Chem. Mater.* **2012**, *24*, 3065-3073.
(19) Eddaoudi, M.; Kim, J.; Rosi, N.; Vodak, D.; Wachter, J.; O'Keeffe, M.; Yaghi, O. M., Systematic Design of Pore Size and Functionality in Isoreticular MOFs and Their Application in Methane Storage. *Science* **2002**, *295*, 469-472.
(20) Ma, D.; Li, Y.; Li, Z., Tuning the Moisture Stability of Metal–Organic Frameworks by Incorporating Hydrophobic Functional Groups at Different Positions of Ligands. *Chem. Commun.* **2011**, *47*, 7377-7379.
(21) Jiang, Z.-R.; Ge, J.; Zhou, Y.-X.; Wang, Z. U.; Chen, D.; Yu, S.-H.; Jiang, H.-L., Coating Sponge with a Hydrophobic Porous Coordination Polymer Containing a Low-Energy CF_3-Decorated Surface for Continuous Pumping Recovery of an Oil Spill from Water. *NPG Asia Materials* **2016**, *8*, e253-e253.

(22) Zhang, W.; Hu, Y.; Ge, J.; Jiang, H.-L.; Yu, S.-H., A Facile and General Coating Approach to Moisture/Water-Resistant Metal–Organic Frameworks with Intact Porosity. *J. Am. Chem. Soc.* **2014**, *136*, 16978-16981.
(23) Mondloch, J. E.; Bury, W.; Fairen-Jimenez, D.; Kwon, S.; DeMarco, E. J.; Weston, M. H.; Sarjeant, A. A.; Nguyen, S. T.; Stair, P. C.; Snurr, R. Q., et al., Vapor-Phase Metalation by Atomic Layer Deposition in a Metal–Organic Framework. *J. Am. Chem. Soc.* **2013**, *135*, 10294-10297.
(24) Kim, I. S.; Borycz, J.; Platero-Prats, A. E.; Tussupbayev, S.; Wang, T. C.; Farha, O. K.; Hupp, J. T.; Gagliardi, L.; Chapman, K. W.; Cramer, C. J., et al., Targeted Single-Site MOF Node Modification: Trivalent Metal Loading Via Atomic Layer Deposition. *Chem. Mater.* **2015**, *27*, 4772-4778.
(25) Ikuno, T.; Zheng, J.; Vjunov, A.; Sanchez-Sanchez, M.; Ortuño, M. A.; Pahls, D. R.; Fulton, J. L.; Camaioni, D. M.; Li, Z.; Ray, D., et al., Methane Oxidation to Methanol Catalyzed by Cu-Oxo Clusters Stabilized in NU-1000 Metal–Organic Framework. *J. Am. Chem. Soc.* **2017**, *139*, 10294-10301.
(26) Beyzavi, M. H.; Vermeulen, N. A.; Howarth, A. J.; Tussupbayev, S.; League, A. B.; Schweitzer, N. M.; Gallagher, J. R.; Platero-Prats, A. E.; Hafezi, N.; Sarjeant, A. A., et al., A Hafnium-Based Metal–Organic Framework as a Nature-Inspired Tandem Reaction Catalyst. *J. Am. Chem. Soc.* **2015**, *137*, 13624-13631.
(27) Noh, H.; Cui, Y.; Peters, A. W.; Pahls, D. R.; Ortuño, M. A.; Vermeulen, N. A.; Cramer, C. J.; Gagliardi, L.; Hupp, J. T.; Farha, O. K., An Exceptionally Stable Metal–Organic Framework Supported Molybdenum(VI) Oxide Catalyst for Cyclohexene Epoxidation. *J. Am. Chem. Soc.* **2016**, *138*, 14720-14726.
(28) Gil-San-Millan, R.; López-Maya, E.; Platero-Prats, A. E.; Torres-Pérez, V.; Delgado, P.; Augustyniak, A. W.; Kim, M. K.; Lee, H. W.; Ryu, S. G.; Navarro, J. A. R., Magnesium Exchanged Zirconium Metal–Organic Frameworks with Improved Detoxification Properties of Nerve Agents. *J. Am. Chem. Soc.* **2019**.
(29) Li, Z.; Schweitzer, N. M.; League, A. B.; Bernales, V.; Peters, A. W.; Getsoian, A. B.; Wang, T. C.; Miller, J. T.; Vjunov, A.; Fulton, J. L., et al., Sintering-Resistant Single-Site Nickel Catalyst Supported by Metal–Organic Framework. *J. Am. Chem. Soc.* **2016**, *138*, 1977-1982.
(30) Korzyński, M. D.; Consoli, D. F.; Zhang, S.; Román-Leshkov, Y.; Dincă, M., Activation of Methyltrioxorhenium for Olefin Metathesis in a Zirconium-Based Metal–Organic Framework. *J. Am. Chem. Soc.* **2018**, *140*, 6956-6960.
(31) Nguyen, H. G. T.; Schweitzer, N. M.; Chang, C.-Y.; Drake, T. L.; So, M. C.; Stair, P. C.; Farha, O. K.; Hupp, J. T.; Nguyen, S. T., Vanadium-Node-Functionalized UiO-66: A Thermally Stable MOF-Supported Catalyst for the Gas-Phase Oxidative Dehydrogenation of Cyclohexene. *ACS Catal.* **2014**, *4*, 2496-2500.
(32) Ji, P.; Manna, K.; Lin, Z.; Feng, X.; Urban, A.; Song, Y.; Lin, W., Single-Site Cobalt Catalysts at New $Zr_{12}(M_3\text{-}O)_8(M_3\text{-}OH)_8(M_2\text{-}OH)_6$ Metal–Organic Framework Nodes for Highly Active Hydrogenation of Nitroarenes, Nitriles, and Isocyanides. *J. Am. Chem. Soc.* **2017**, *139*, 7004-7011.
(33) Manna, K.; Ji, P.; Greene, F. X.; Lin, W., Metal–Organic Framework Nodes Support Single-Site Magnesium–Alkyl Catalysts for Hydroboration and Hydroamination Reactions. *J. Am. Chem. Soc.* **2016**, *138*, 7488-7491.
(34) Otake, K.-i.; Cui, Y.; Buru, C. T.; Li, Z.; Hupp, J. T.; Farha, O. K., Single-Atom-Based Vanadium Oxide Catalysts Supported on Metal–Organic Frameworks: Selective Alcohol Oxidation and Structure–Activity Relationship. *J. Am. Chem. Soc.* **2018**, *140*, 8652-8656.
(35) Jiao, L.; Jiang, H.-L., Metal-Organic-Framework-Based Single-Atom Catalysts for Energy Applications. *Chem* **2019**, *5*, 786-804.
(36) Li, D.; Xu, H.-Q.; Jiao, L.; Jiang, H.-L., Metal-Organic Frameworks for Catalysis: State of the Art, Challenges, and Opportunities. *EnergyChem* **2019**, *1*, 100005.
(37) Li, Z.; Peters, A. W.; Platero-Prats, A. E.; Liu, J.; Kung, C.-W.; Noh, H.; DeStefano, M. R.; Schweitzer, N. M.; Chapman, K. W.; Hupp, J. T., et al., Fine-Tuning the Activity of Metal–Organic Framework-Supported Cobalt Catalysts for the Oxidative Dehydrogenation of Propane. *J. Am. Chem. Soc.* **2017**, *139*, 15251-15258.

(38) Kung, C.-W.; Mondloch, J. E.; Wang, T. C.; Bury, W.; Hoffeditz, W.; Klahr, B. M.; Klet, R. C.; Pellin, M. J.; Farha, O. K.; Hupp, J. T., Metal–Organic Framework Thin Films as Platforms for Atomic Layer Deposition of Cobalt Ions to Enable Electrocatalytic Water Oxidation. *ACS Applied Materials & Interfaces* **2015**, *7*, 28223-28230.
(39) Hod, I.; Deria, P.; Bury, W.; Mondloch, J. E.; Kung, C.-W.; So, M.; Sampson, M. D.; Peters, A. W.; Kubiak, C. P.; Farha, O. K., et al., A Porous Proton-Relaying Metal-Organic Framework Material That Accelerates Electrochemical Hydrogen Evolution. *Nat. Commun.* **2015**, *6*, 8304.
(40) Furukawa, H.; Gándara, F.; Zhang, Y.-B.; Jiang, J.; Queen, W. L.; Hudson, M. R.; Yaghi, O. M., Water Adsorption in Porous Metal–Organic Frameworks and Related Materials. *J. Am. Chem. Soc.* **2014**, *136*, 4369-4381.
(41) Deria, P.; Mondloch, J. E.; Tylianakis, E.; Ghosh, P.; Bury, W.; Snurr, R. Q.; Hupp, J. T.; Farha, O. K., Perfluoroalkane Functionalization of NU-1000 via Solvent-Assisted Ligand Incorporation: Synthesis and CO_2 Adsorption Studies. *J. Am. Chem. Soc.* **2013**, *135*, 16801-16804.
(42) Bon, V.; Senkovska, I.; Weiss, M. S.; Kaskel, S., Tailoring of Network Dimensionality and Porosity Adjustment in Zr- and Hf-Based MOFs. *CrystEngComm* **2013**, *15*, 9572-9577.
(43) Wu, H.; Chua, Y. S.; Krungleviciute, V.; Tyagi, M.; Chen, P.; Yildirim, T.; Zhou, W., Unusual and Highly Tunable Missing-Linker Defects in Zirconium Metal–Organic Framework UiO-66 and Their Important Effects on Gas Adsorption. *J. Am. Chem. Soc.* **2013**, *135*, 10525-10532.
(44) Planas, N.; Mondloch, J. E.; Tussupbayev, S.; Borycz, J.; Gagliardi, L.; Hupp, J. T.; Farha, O. K.; Cramer, C. J., Defining the Proton Topology of the Zr_6-Based Metal–Organic Framework NU-1000. *J. Phys. Chem. Lett.* **2014**, *5*, 3716-3723.
(45) Kobayashi, T.; Sasaki, T.; Takagi, I.; Moriyama, H., Solubility of Zirconium(IV) Hydrous Oxides. *J. Nucl. Sci. Technol.* **2007**, *44*, 90-94.
(46) Brito, F.; Ascanio, J.; Mateo, S.; Hernández, C.; Araujo, L.; Gili, P.; Martín-Zarza, P.; Domínguez, S.; Mederos, A., Equilibria of Chromate(VI) Species in Acid Medium and ab Initio Studies of These Species. *Polyhedron* **1997**, *16*, 3835-3846.
(47) Troya, D., Reaction Mechanism of Nerve-Agent Decomposition with Zr-Based Metal Organic Frameworks. *J. Phys. Chem. C* **2016**, *120*, 29312-29323.
(48) Dean, J. A., *Lange's Handbook of Chemistry*; New york; London: McGraw-Hill, Inc., 1999.
(49) Helm, L.; Merbach, A. E., Water Exchange on Metal Ions: Experiments and Simulations. *Coord. Chem. Rev.* **1999**, *187*, 151-181.
(50) Wang, S.; Petzold, V.; Tripkovic, V.; Kleis, J.; Howalt, J. G.; Skúlason, E.; Fernández, E. M.; Hvolbæk, B.; Jones, G.; Toftelund, A., et al., Universal Transition State Scaling Relations for (De)Hydrogenation over Transition Metals. *PCCP* **2011**, *13*, 20760-20765.
(51) Serre, C.; Millange, F.; Thouvenot, C.; Noguès, M.; Marsolier, G.; Louër, D.; Férey, G., Very Large Breathing Effect in the First Nanoporous Chromium(III)-Based Solids: MIL-53 or $Cr^{iii}(OH)\cdot\{O_2C{-}C_6H_4{-}CO_2\}\cdot\{HO_2C{-}C_6H_4{-}CO_2H\}_X\cdot H_2O_y$. *J. Am. Chem. Soc.* **2002**, *124*, 13519-13526.

TOC Graphic

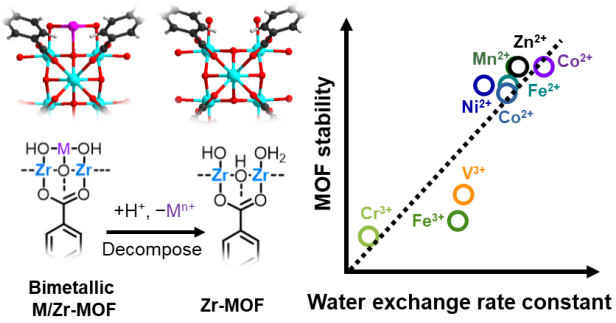
HO-M-OH
--Zr-O-Zr---
+H+, −Mn+
Decompose
HO H OH2
--Zr-O-Zr--
Bimetallic
M/Zr-MOF
Zr-MOF
MOF stability
Water exchange rate constant
Zn2+
Mn2+
Co2+
Fe2+
Ni2+
Co2+
V3+
Cr3+
Fe3+